Supporting Information

Biofunctionalized plants as diverse biomaterials for human cell culture

Gianluca Fontana, Joshua Gershlak, Michal Adamski, Jae-Sung Lee, Shion Matsumoto, Hau D. Le, Bernard Binder, John Wirth, Glenn Gaudette, William L. Murphy *

Supplementary Experimental Section

Sample preparation for Scanning Electron Microscope (SEM) imaging: Immediately after collection, the samples were immersed in a buffered solution of 2% paraformaldehyde (PFA) in 1X PBS for maximum 30 minutes. A more extensive fixation was obtained by incubating the samples in 1.5% Glutaraldehyde in freshly prepared 70 mM sodium Cacodylate buffer pH 7.4. The samples were then rinsed in 70 mM Sodium Cacodylate buffer with the addition of 2.5% sucrose and dehydrated by immersion in a graduated series of ethanol in H_2O and hexamethyldisilazane (HDMS) in ethanol baths of respectively 30, 50, 80 and 95%. The samples were left to dry on the sample holder and then gold sputter coated prior imaging in SEM.

Quantification of water retention: Lyophilized plant's stems were weighed dry (n=4) and then immersed in 2 mL water for 1 hour at room temperature. Successively, the wet stems were weighed a second time and the weight difference was considered as the amount of water retained by the stems.

Pore size quantification: Normal and decellularized stems were characterized using SEM. Images were analyzed using the software ImageJ and the diameter of at least 50 pores per stem was measured from at least 3 different images.

Cell imaging: Calcein staining was used to perform live-cell staining. Samples were incubated for 30 minutes in 10mM calcein (Life Technologies™, C3099) and subsequently washed in PBS 1X. Each sample was imaged using a fluorescence microscope. Cell cytoskeleton instead, was stained using phalloidin. Samples were incubated for 2 hours in rhodamine–phalloidin (Cytoskeleton Inc, PHDR1) following directions from the supplier's protocol and 10 min in 4′,6-diamidino-2-phenylindole (DAPI) to stain the nuclei. Images were acquired by using a fluorescence microscope.

Quantification of cellular orientation: To quantify cellular orientation we assumed that nuclear shape is related to cell shape as the link between these two features has been highlighted in a number of studies already. Nuclear shape was assessed by analyzing images of DAPI-stained cells using the software cellProfiler. The captured images were rotated following the direction of the topographical features of the stems (monolayer controls were rotated randomly). The background of the images was subtracted and the threshold was set manually for each individual image to avoid the quantification of artifacts. Also, each object was filtered using size criteria, only objects with a size comprised between 1 and 50 μm were counted. The software then measured the angle between the longest side of cell's nuclei and the topographical features of the stems in such a way that 0° corresponded to perfect alignment. Only cells oriented within a specific angle range (20°, 30° and 40°) were counted and normalized over the total number of cells.

Quantification of cellular metabolic activity: Cellular metabolic activity was assessed using the CellTiter-Blue® assay (Promega, G8081) and following the manufacture's protocol. Briefly, a 24

well plate was used to culture cell-laden stems, 40 µL of CellTiterBlue® were added in each well and incubated at 37°C for 24 hours. The following day, 100 µL were collected from each sample and transferred to a black 96 well plate. The fluorescence signal was recorded ($560_{ex}/590_{em}$) using a multiplate reader Even though stems were cut to the same length, they had different diameters, thereby having different seeding surfaces. Cells had the tendency to grow on the outer part of the stems, for this reason we decided to consider only the external surface of the stems as "seeding area". The seeding area was calculated using the formula: $A=2\pi rh+2\pi r2$ because of the cylindrical shape of the stems.

Histological Analysis: Stems were cut into approximately 1 cm length pieces. Samples were fixed overnight in an ATP-1 automatic tissue processor (Triangle Biomedical Sciences, North Carolina) prior to being paraffin embedded. Embedded tissues were sectioned in 14 µm slices. Sections were stained using Sass's Safranin-O and Fast Green. In short, sections were stained for 1 hour in aqueous 1% (w/v) Safranin-O and then rinsed in deionized water for 5 minutes. Tissues were then dehydrated serially in 70% and then 95% ethanol for 3 minutes each. Sections were then dipped for 10 seconds in Fast Green FCF (0.1% w/v in 95% ethanol). After dipping, sections were washed of excess stain in two changes of 100% ethanol for 2 minutes per change and then cleared in two changes of xylene for 2 minutes per change. Samples were then mounted with a coverslip and sealed with Cytoseal XYL (Thermo Fisher Scientific, Waltham, MA). Images of tissue sections were visualized using a DMLB2 upright microscope (Leica Microsystems, Buffalo Grove, IL). Further stains performed on cell-laden stems were H&E and Masson's Trichrome.

DNA Quantification: Native and decellularized parsley stems were cut into 1 cm long sections and placed into microcentrifuge tubes. Tissues were snap-frozen by being dropped into liquid nitrogen for 1 minute. Frozen tissue pieces were ground with a mortar and pestle and then further processed by being pulled through a 22-gauge syringe needle. Samples were further broken up through sonication. DNA was quantified from pulverized samples using a CyQUANT Direct Cell Proliferation Assay (Thermo Fisher, Waltham, MA). Concentrations were determined using a Victor3 spectrophotometer (Perkin Elmer, Waltham, MA)

NMR analysis of conjugated peptide: The conjugation of dopamine to RGD peptide was verified with 1H nuclear magnetic resonance (NMR) spectroscopy. 1H NMR spectra were recorded using using Bruker Avance III (500 MHz) in D2O supplemented with 4,4-dimethyl-4-silapentane-1-sulfonic acid (DSS) as an internal standard.

Mechanical Testing: Normal and mineralized parsley stems were cut into 2 mm long sections. The ends of the stem sections were sealed with silicon glue between two pieces of vellum paper in order to ensure a strong grip and uniform strain. Stems were uniaxially stretched at a constant rate of 5 mm/min in an ElectroPuls E1000 tester (Instron Corp., Norwood, MA). Maximum tangent modulus, ultimate tensile strength, and strain at failure were calculated. Maximum tangent modulus was established by fitting a line to the maximal sloped linear region of the stress-strain graph. Ultimate tensile strength and strain at failure were calculated from the generated stress-strain graphs.

Supplementary Figures

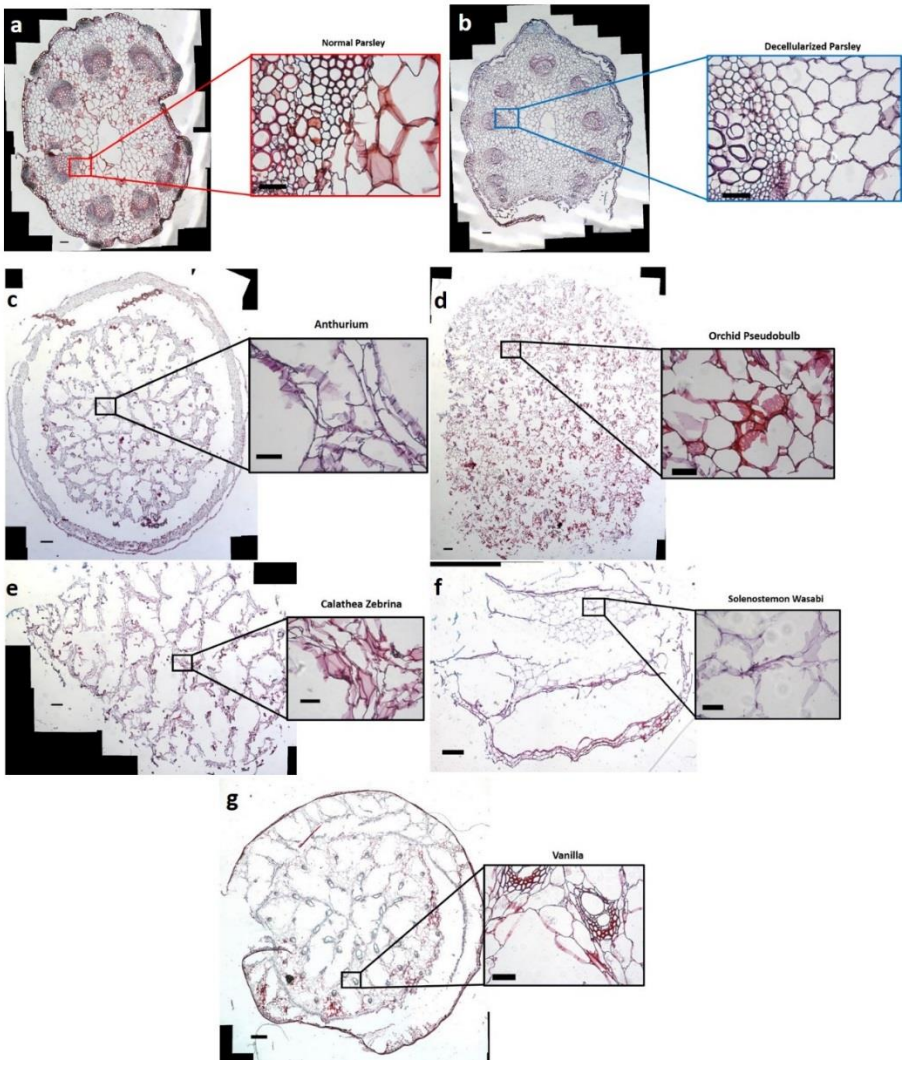

Figure S1: Histology characterization reveals effective decellularization. Sass's Safranin-O (it stains nuclei and chromosomes red) and Fast Green (it stains cytoplasms and cell walls bright green) staining of sections of plant tissues show effective decellularization of plant stems. **a,** section of normal parsley. **b,** section of decellularized parsley stem. **c,** section of decellularized *Anthurium waroqueanum* stem. **d,** Section of orchid's pseudobulb. **e,** section of *Calathea zebrina* stem. **f,** section of Solenostemon stem. **g,** Section of Vanilla stem. Scalebars 500 µm and 50 µm in the magnified images.

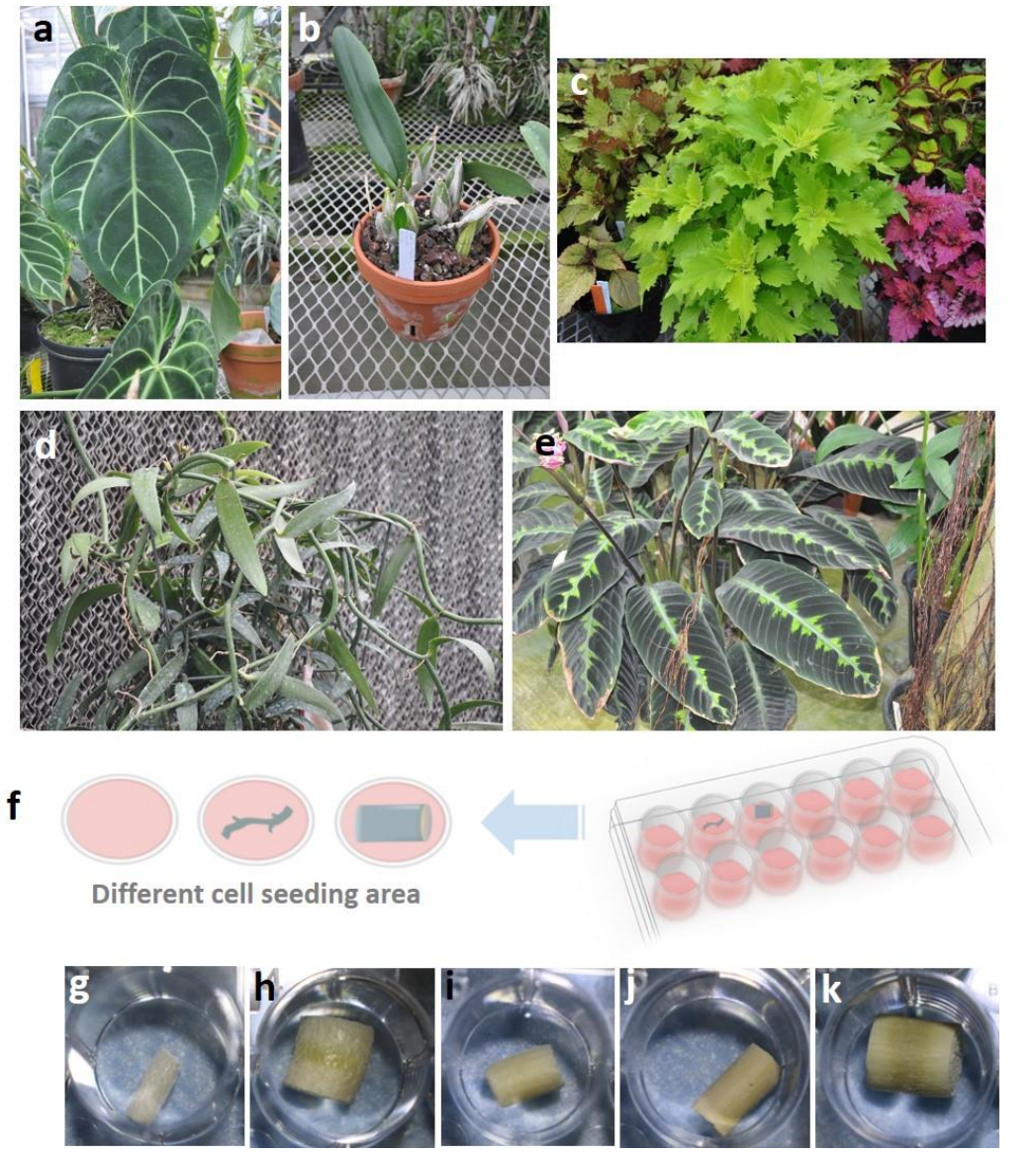

Figure S2: Plants used for the study. a, *Anthurium magnificum*. **b,** *Laelia ancepts* (orchid). **c,** Solenostemon. **d,** Vanilla. **e,** *Calathea zebrina*. **f**, Schematic depicting the differences in cell seeding areas in stems originating from different plants. **g**, parsley stem. **h**, *Anthurium waroqueanum* stem. **i**, *Calathea zebrina* stem. **j**, Bamboo stem. **k**, Vanilla stem.

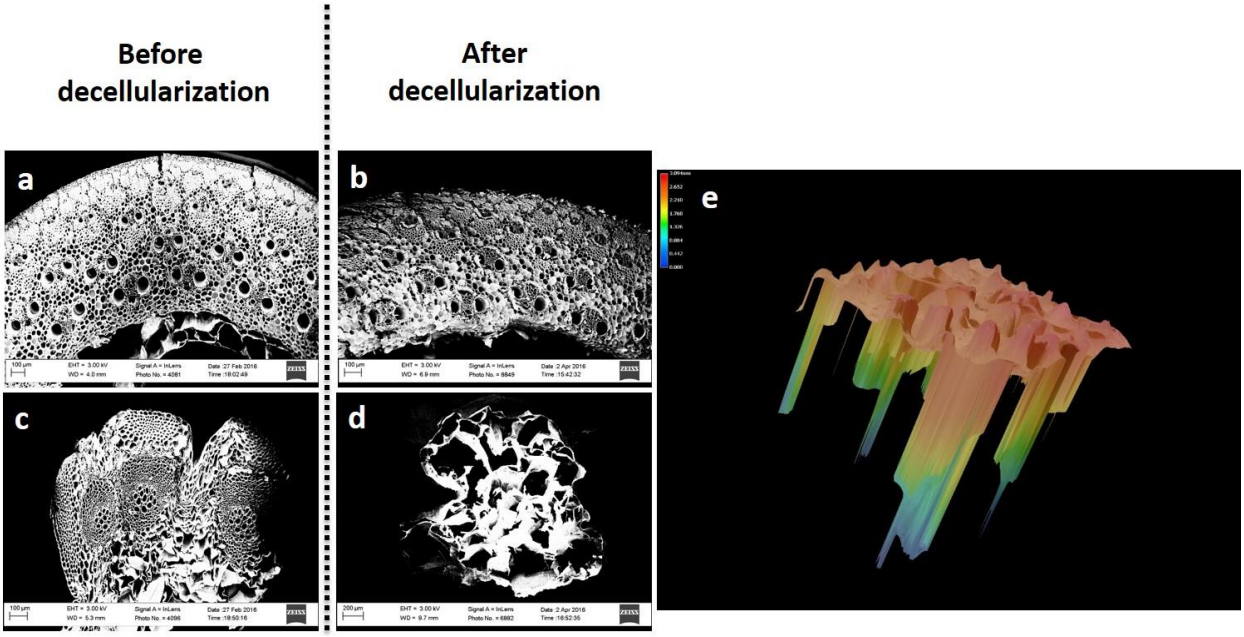

Figure S3: Comparison of structural changes before and decellularization. a-b, SEM cross-sections of bamboo stems respectively before and after decellularization. No major structural changes occurred and the pores size in both stems was comparable. **c-d,** SEM cross-sections of parsley stems before and after decellularization respectively. In this case, pores diameter was significantly enlarged in decellularized stems. **e,** 3D representation of pores depth in a *Anthurium waroqueanum* stem. The total length of the stem was 7 mm and the deepest pore measured about 3 mm in depth. Imaging performed using the digital microscope VHX-5000 by Keyence.

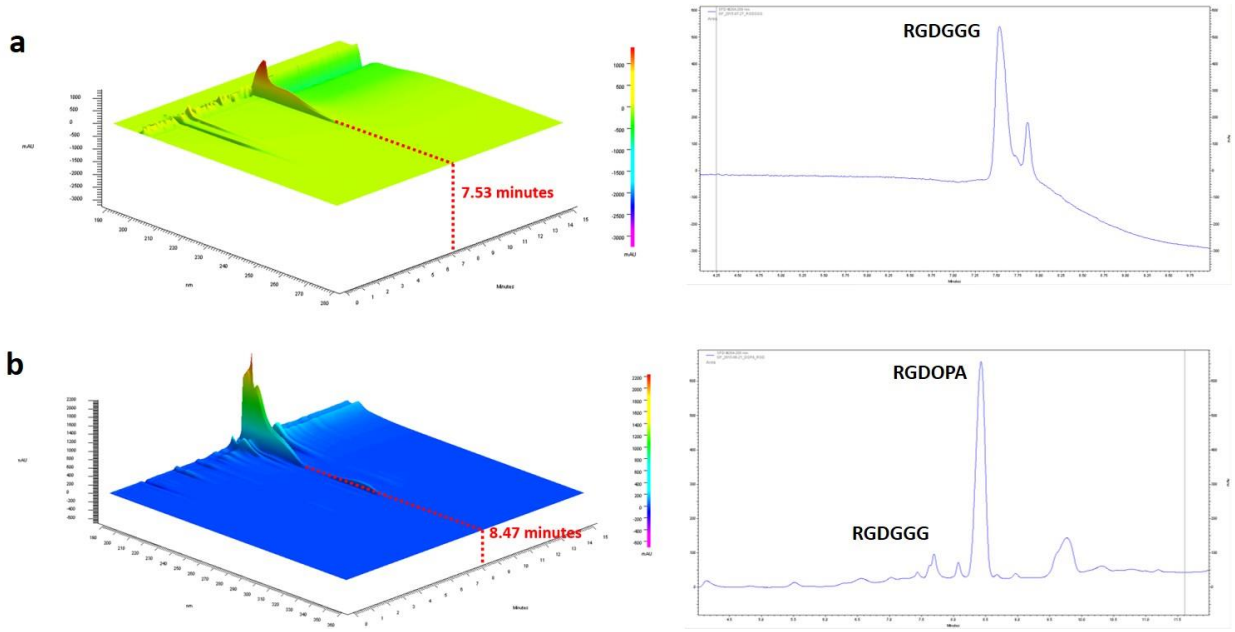

Figure S4: High purity of RGDOPA after dialysis. a, HPLC spectra of the peptide RGDGGG shows a single major peak indicative of high purity. The elution time for the peptide alone was 7.53 minutes. **b,** HPLC spectra of the peptide RGDGGG conjugated with dopamine (RGDOPA). Following dialysis there seems to be only minimal presence of un-conjugated peptide and the elution time of the main peak is 8.47 minutes, a shift of about 1 minute relative to the un-conjugated peptide.

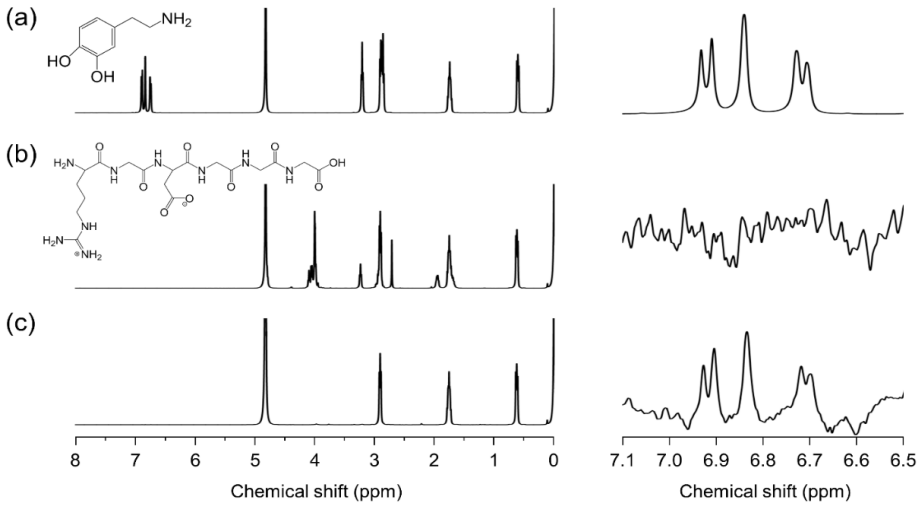

Figure S5 NMR confirms the presence of dopamine in RGDOPA: ^{1}H NMR spectra of (a) dopamine, (b) RGDGGG and (c) RGDOPA. Shown in right column are the enlarged spectra in the range of 6.5 to 7.1 ppm to monitor the presence of aromatic protons.

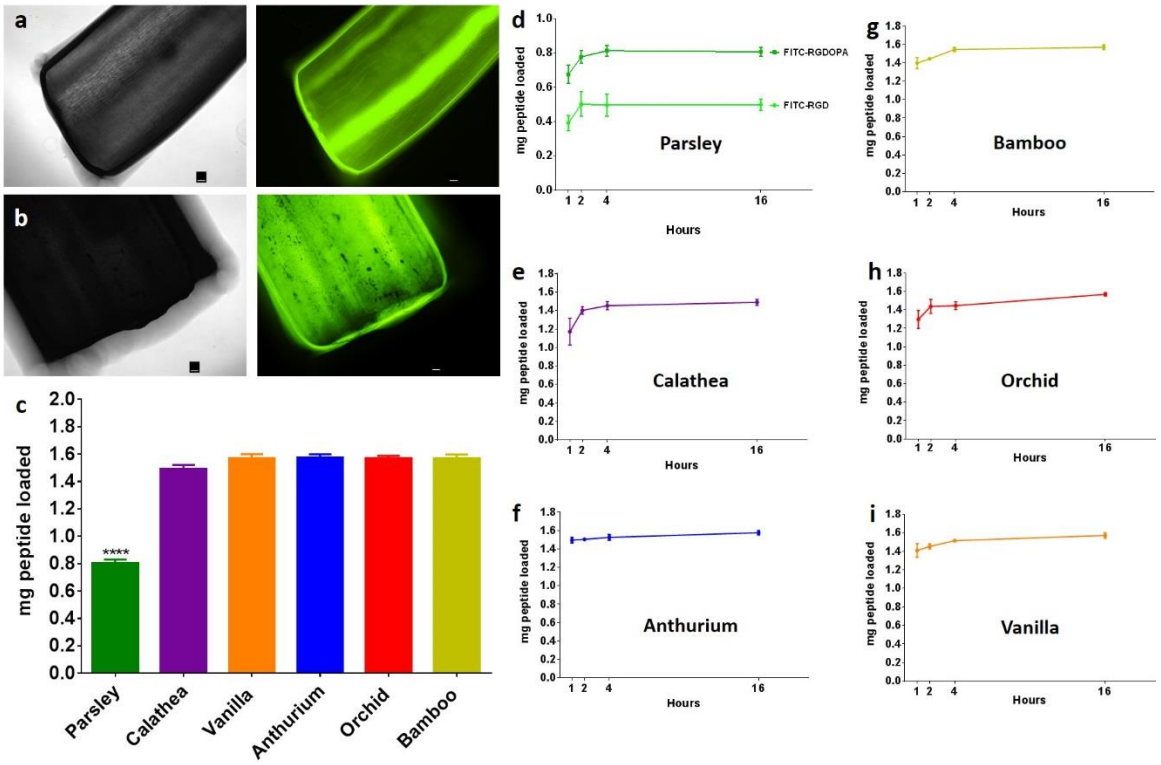

Figure S6 Effective RGDOPA functionalization of plant stems: To assess if DOPA-conjugated RGD peptides (RGDOPA) are effective in functionalizing plant stems a FITC-labelled RGD peptide was used and its binding kinetics to the stems was monitored for a period of 16 hours. **a,** Parsley stem functionalized with FITC-RGD, scalebars 100 µm; **b,** Parsley stem functionalized with FITC-RGDOPA, scalebars 100 µm; **c,** Quantification of the total peptide bound to different stems after 16 hours of incubation; **d,** Comparison of loading kinetics of FITC-RGD and FITC-RGDOPA. The peptide conjugation to dopamine increases significantly its ability to bind to the plant stems. **e-i,** FITC-RGDOPA loading kinetics respectively on, *Calathea zebrina*, *Anthurium waroqueanum*, bamboo, orchid's pseudobulbs, and vanilla stems.

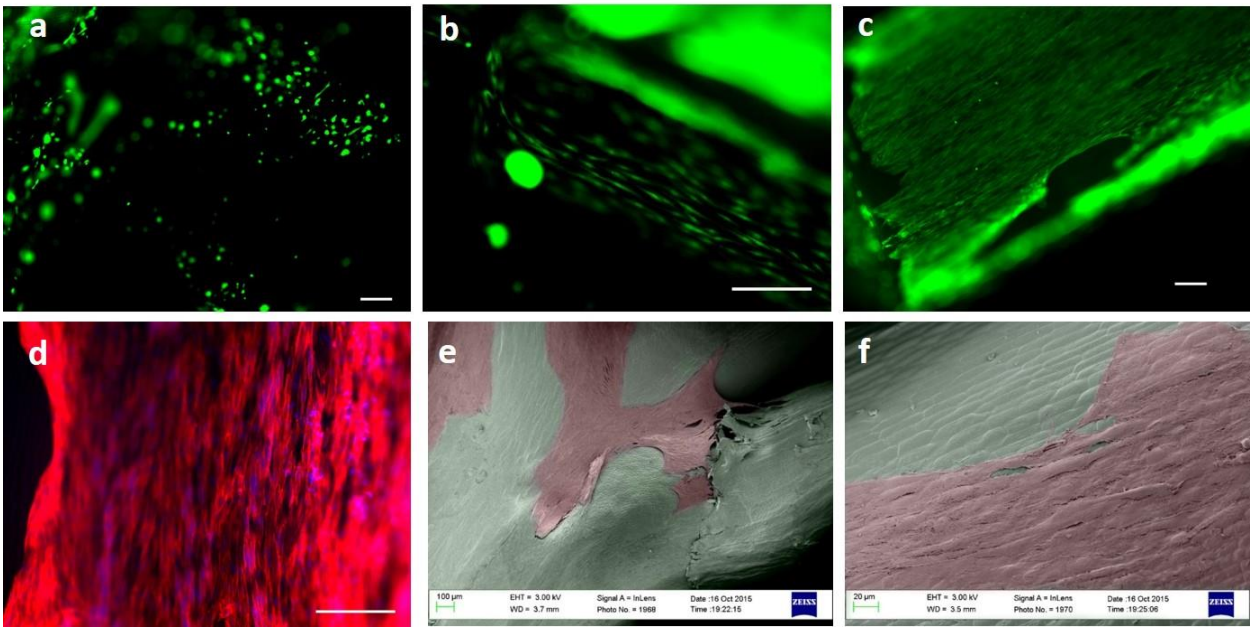

Figure S7: hDF seeded on RGDOPA-coated *Impatiens capensis* stems. a-c, Calcein staining of hDF cultured for 2 days on *Impatiens capensis* stems respectively: non treated (a), RGDOPA-coated (b) and RGDOPA-coated and cultured for 2 weeks (c). When seeded on treated stems, cells acquired the typical spindle-shape of adhering cells, while when seeded on non-treated stems they were rounded, hallmark of low interaction with the surface of plant tissues. After 2 weeks of culture (c) there were visibly more cells on the stem compared to 2 days (b) indicating cell expansion. Scalebars 250 µm. **d,** Rhodamine-phalloidine staining of actin filaments (red) and dapi staining of nuclei (blue) of hDF cultured on *Impatiens capensis* stems for 2 weeks. Scalebar 250 µm. **e-f,** Color-enhanced SEM micrographs displaying hDF (pink) growing on the surface of *Impatiens capensis* stems (green).

Table S1: BET analysis of decellularized stems

Sample	Total Surface Area (m^2/g)	Average Pore Diameter (nm)	Total Pore volume (cc/g)
Parsley (non-coated)	1869	4.24	1.981
Parsley (RGDOPA)	1768	4.18	1.85
Parsley (mineralized)	523.5	4.22	0.522
Bamboo (non-coated)	46.32	3.93	0.0455
Bamboo (RGDOPA)	40.41	3.97	0.0401
Vanilla (RGDOPA)	193.9	3.82	0.185
Calathea (RGDOPA)	142.4	3.92	0.14
Orchid (non-coated)	271.5	4.23	0.28
Orchid (RGDOPA)	212.5	4.76	0.253
Anthurium (RGDOPA)	43.34	4.53	0.049

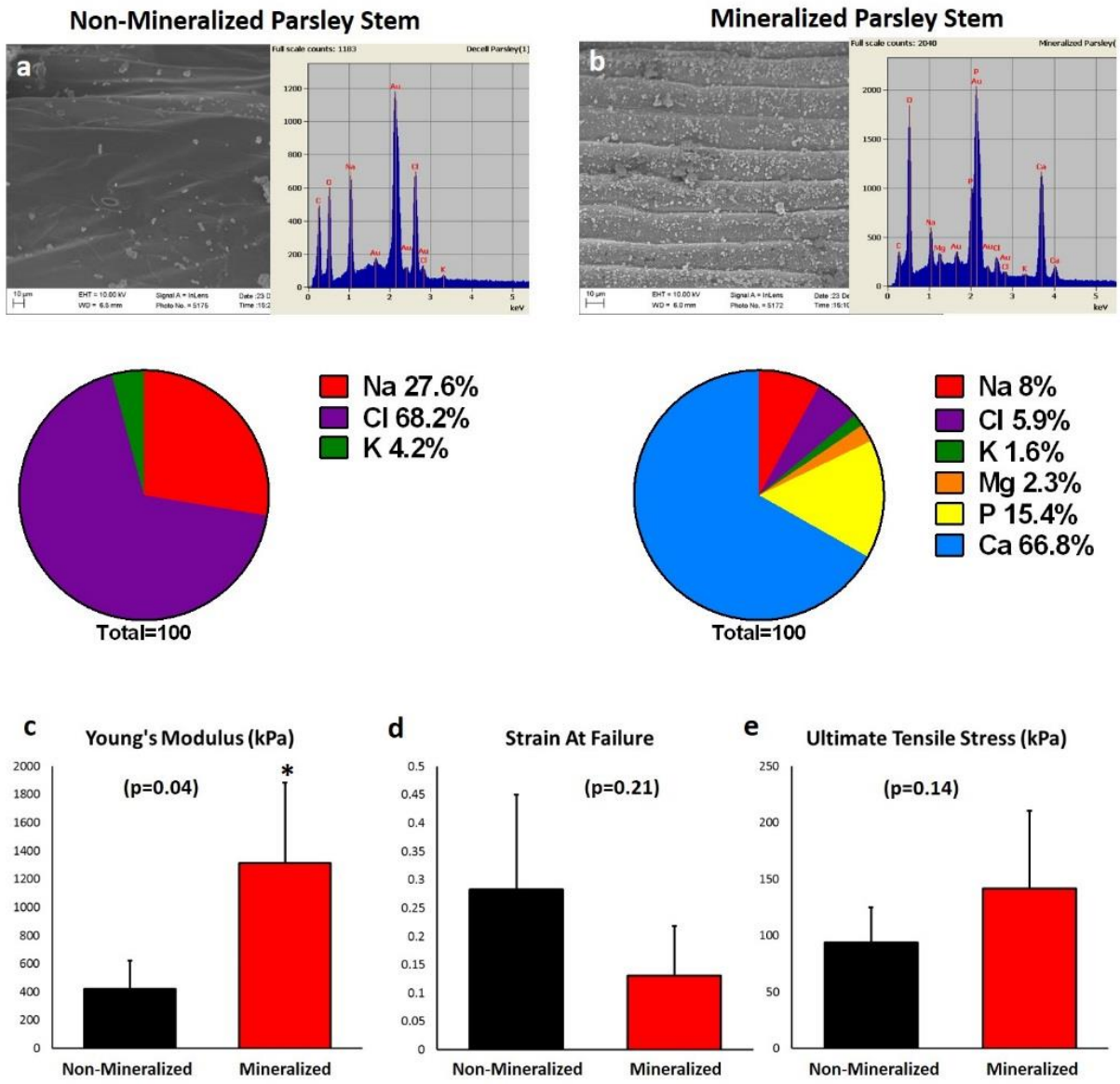

Figure S8 Effects of mineralization on parsley stems: a-b, SEM micrograph and EDS analysis of a parsley stem non-mineralized (a) and mineralized (b). **c-e,** mechanical testing revealed that mineralization of parsley stems increased their young's modulus (c) but it did not have significative effects on their strain at failure (d) or tensile stress (e).

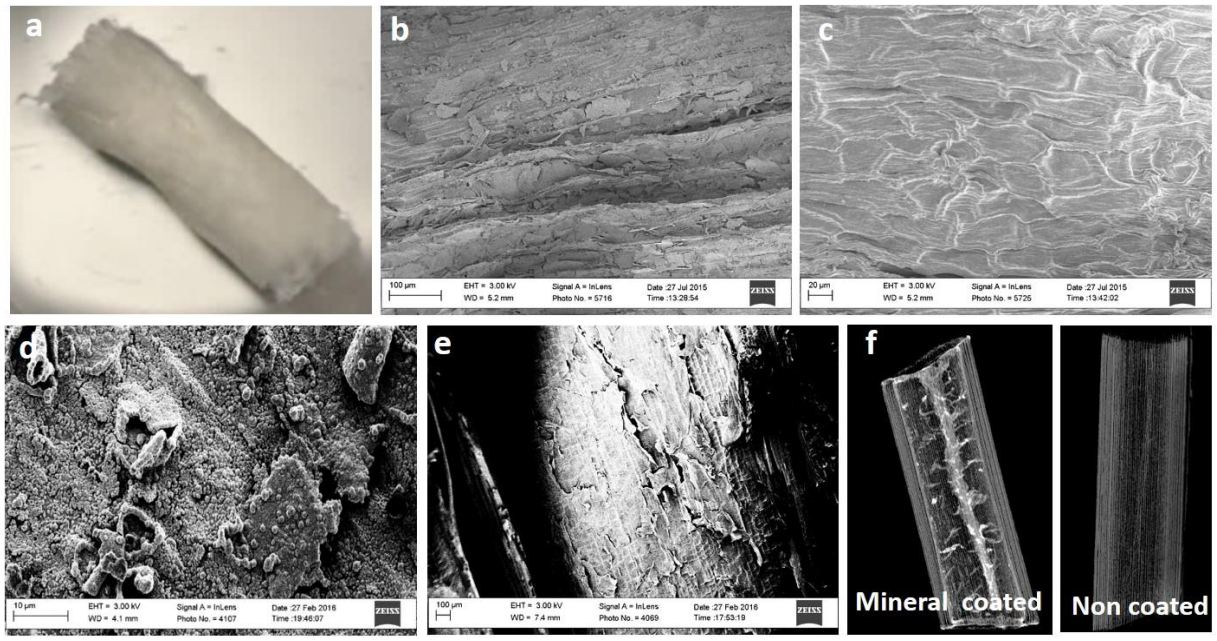

Figure S9: Mineralization of plant's stems. a, Mineralized parsley stem. **b-c,** SEM micrographs comparing the surface of mineralized and non-mineralized parsley stems respectively. The surface of mineralized parsley stems is characterized by the presence of mineral flakes, normal parsley instead, shows smooter surfaces typical of cuticle tissue. **d-e,** SEM micrographs comparing the surface of mineralized and non-mineralized bamboo stems. Mineral-coated bamboo stems display rough surfaces, normal bamboo instead show very smooth surfaces. **F,** Faxitron images of respectively coated and non coated bamboo stems.

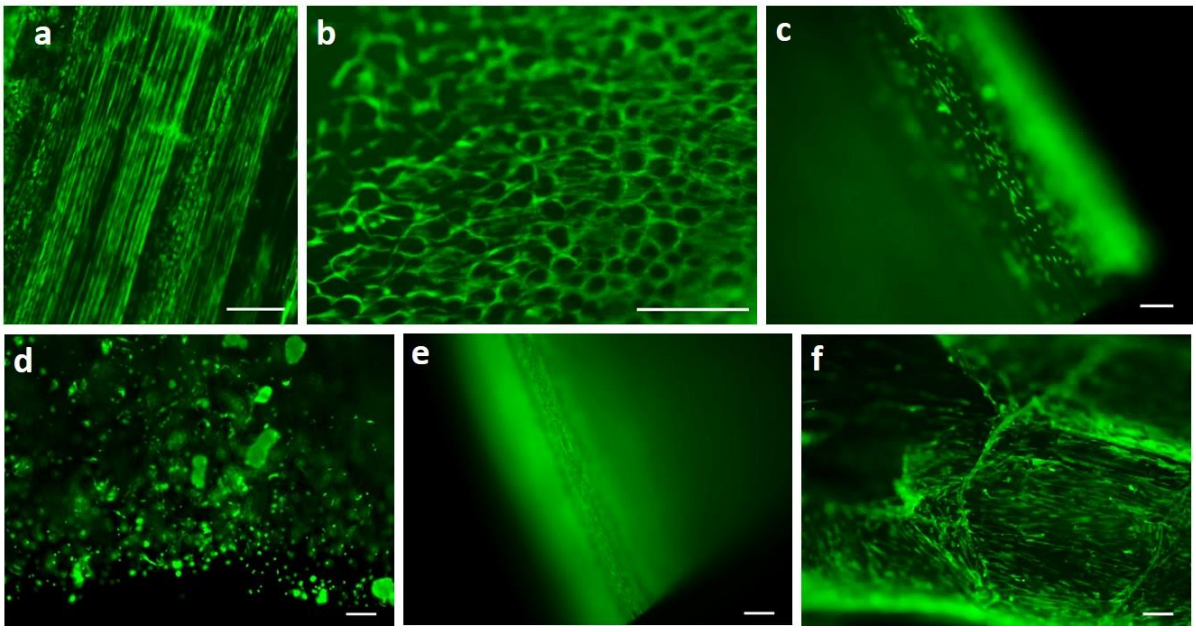

Figure S10 Calcein staining of hDF seeded on different stems: Calcein staining of hDF cultured for 7 days on a variety of RGDOPA-coated stems show that cells were able to adhere and be viable on all plant scaffolds. Cells were seeded respectively on: **a,** Solenostemon. **b,** *Anthurium waroqueanum*. **c,** Bamboo. **d,** Orchid's pseudobulb. **e,** Vanilla. **f,** Parsley. Scalebars 250 µm.

Table S2: Seeding area of decellularized stems.

Sample	Seeding Area (mm^2)
Monolayer control	254.34
Anthurium waroqueanum	293.41 ± 34.52
Vanilla	318.05 ± 28.09
Solenostemon	119.77 ± 9.09
Orchid's Pseudobulb	314.27 ± 47.29
Parsley	73.22 ± 12.39
Mineralized Parsley	91.75 ± 17.47
Calathea zebrina	172.66 ± 31.43

(Each stem had a cylindrical shape, therefore the seeding area was calculated using the following formula: $A=2\pi rh+2\pi r^2$).

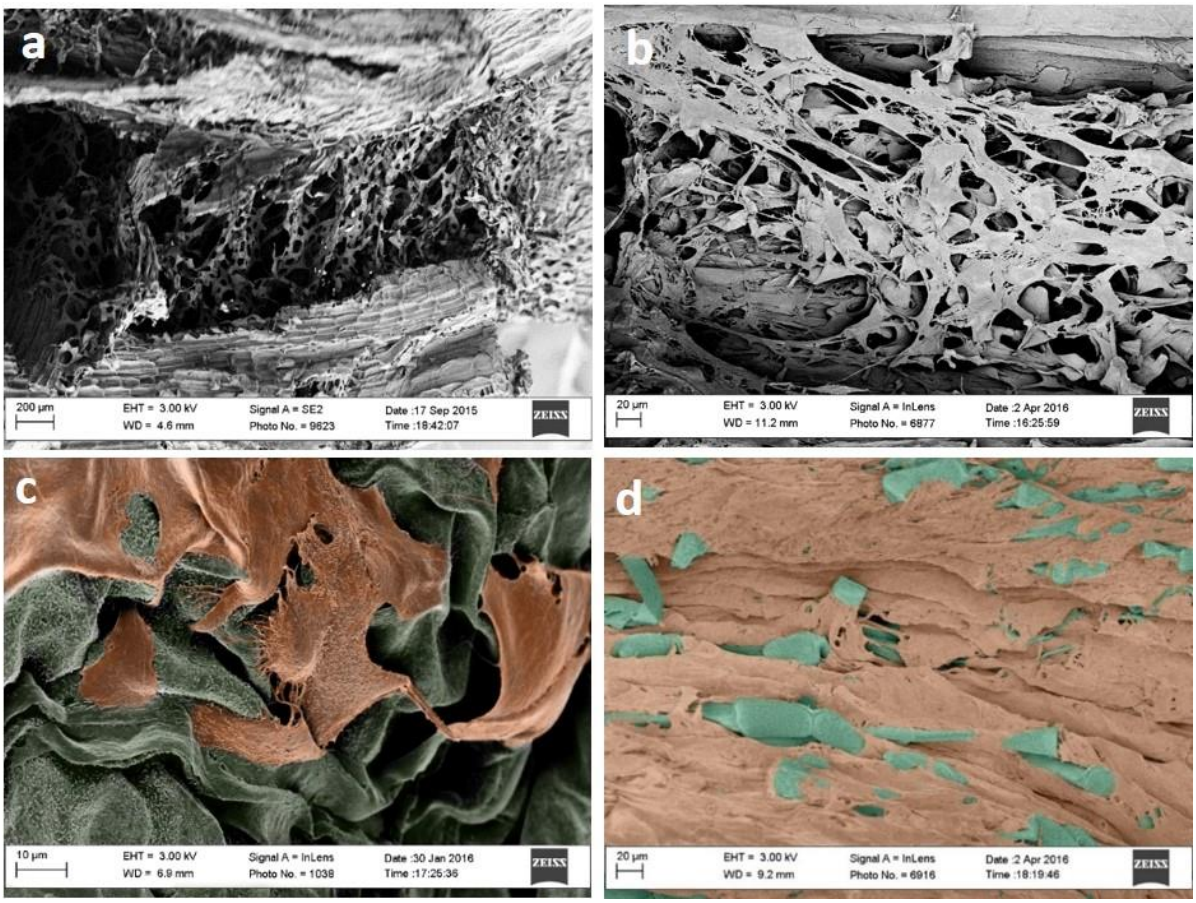

Figure S11: hDF can adhere on biofunctionalized plant tissues. a, SEM micrograph showing a sideview of a *Schoenoplectus tabernaemontani* stem. This plant appears to have several internal layers that increase its surface area and maximize the plant's ability to exchange oxygen and nutrients. **b,** SEM micrograph displaying hDF seeded in a *Schoenoplectus tabernaemontani* stem. The high surface area of this stem may allow considerable cell expansion. **c-d**, color-enhanced SEM micrographs of hDF seeded respectively on a summer lilac leaf (c) and on Solenostemon stems (d).

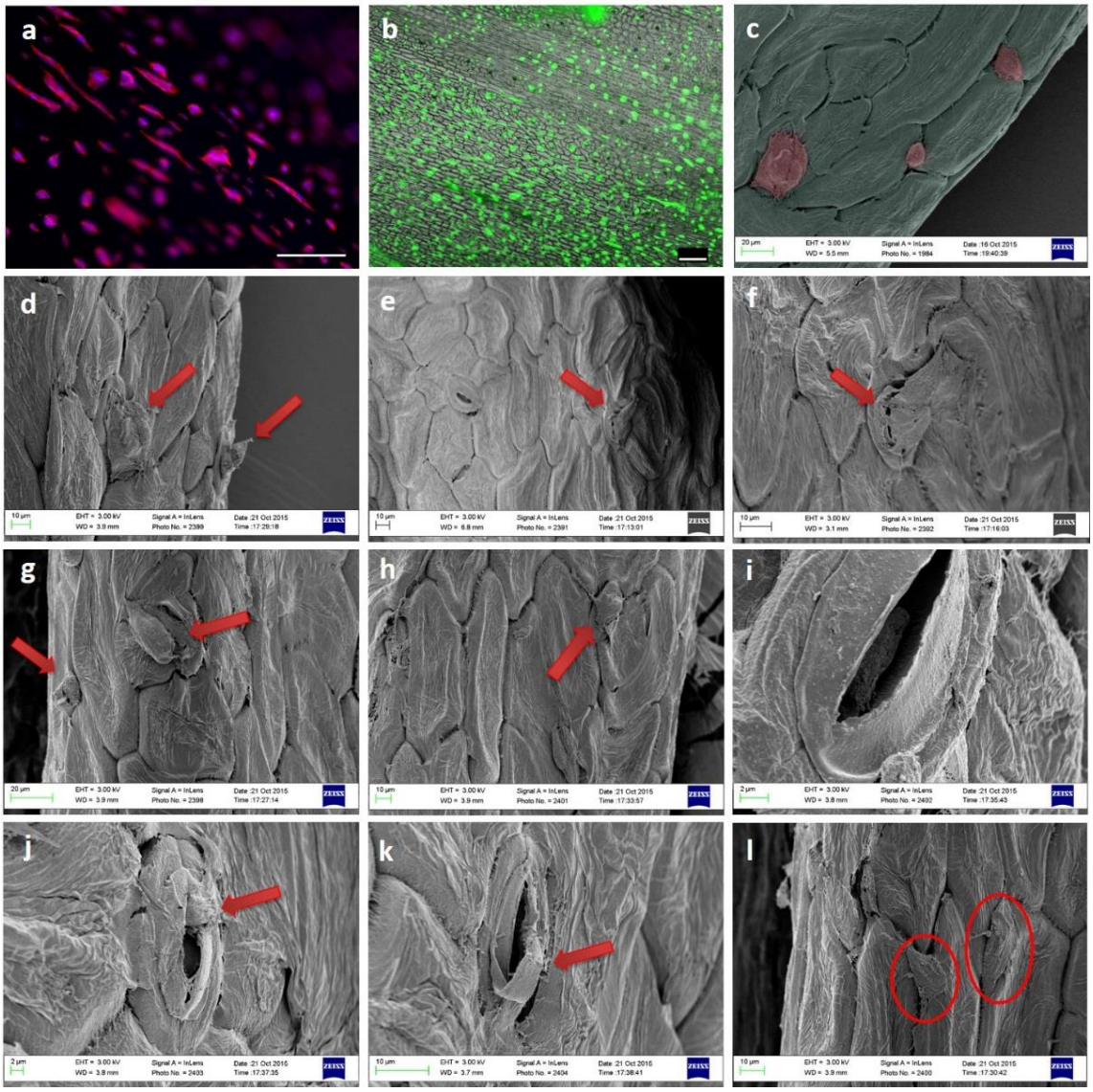

Figure S12: Interplay between hDF and structural cues of parsley stems: a, Rhodamine-phalloidine staining of actin filaments (red) and dapi staining of nuclei (blue) of hDF seeded on parsley stems. Cells appeared to be polarized, following the topographical orientation of the stem. **b,** calcein live-staining of hDF seeded on parsley stems for 7 days. Scalebars 250 µm. **c,** Color-enhanced SEM micrograph of hDF cultured on parsley stems. Cells seemed to grow in proximity of concave areas of the stem. **d-k,** panel of SEM images showing a number of cases in which hDF (highlighted with red arrows) were found in proximity of the stomata on parsley stems **I,** SEM micrograph showing hDF adhering on concave areas on a parlsey stem.

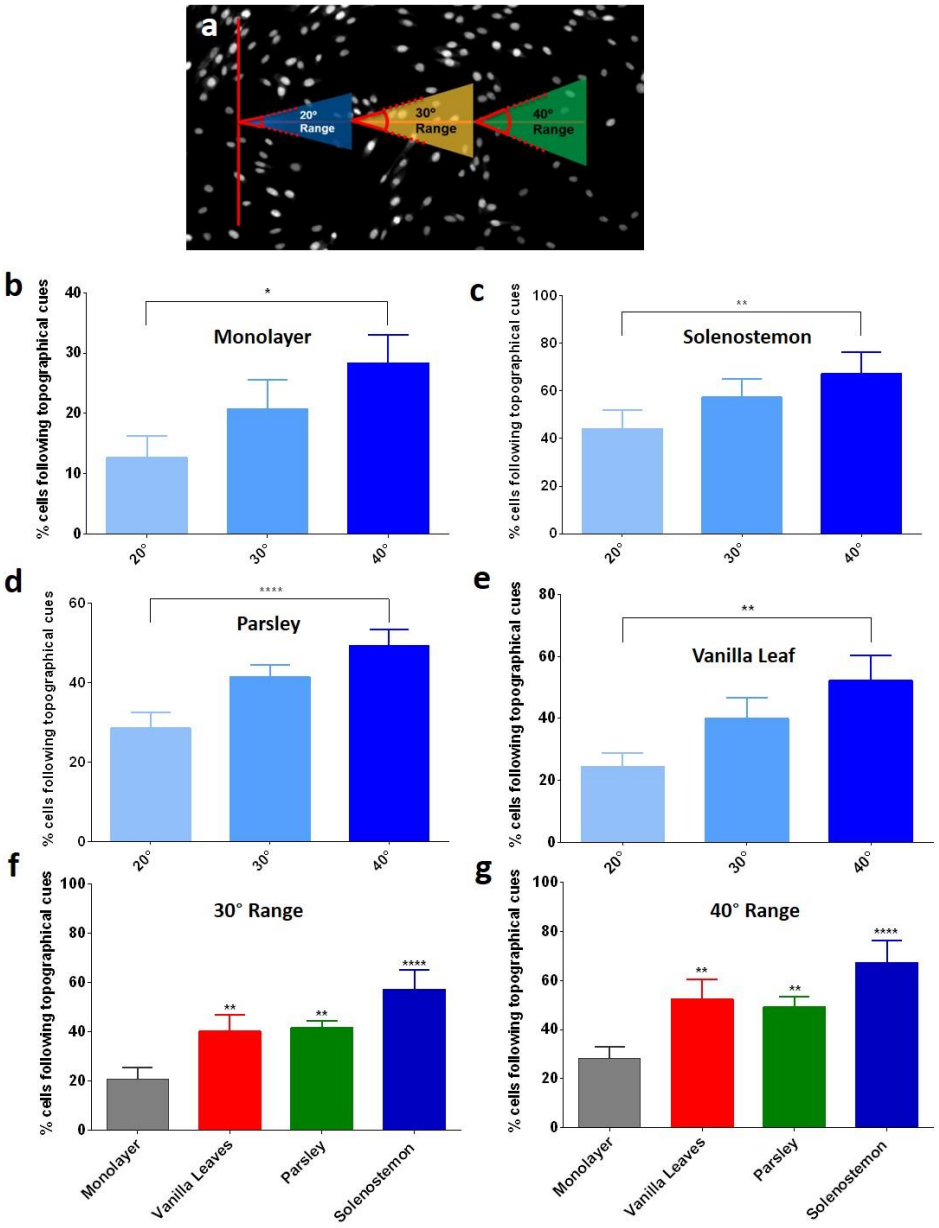

Figure S13: hDF orientation influenced by the topographical cues of plant tissues. a, Conceptual illustration of the method used for the quantification of OA. In the case of plant tissues, an axis was drawn following the topography of the stems and the software cellProfiler was used to measure the angle between the longest side of the cell's nuclei and the axis. Only cells oriented within certain angle ranges were counted and normalized over the total number of cells. **b-e,** quantification of cellular orientation respectively on monolayer (b), Solenostemon (c), Parsley (d) and Vanilla leaf (e). Clearly, the data show that increasing the angle range corresponds to an increase of percentage of cells oriented in the same direction. Using a range of 40 degrees we found that 30% of the cells are oriented the same way in monolayer, 75% in Solenostemon, 50% in Parsley and 50% in Vanilla leaf. Monolayer (750 cells, 3 samples), Solenostemon (1792 cells, 4 samples), Parsley (617 cells, 4 samples), Vanilla leaves (864 cells, 3 samples) $p<0.05$ one-way ANOVA followed by Tukey's multiple comparisons test. **f-g,** Quantification of cellular

orientation comparing samples with one another. Regardless of the angle range considered, significantly more cells follow the same orientation in Solenostemon. Parsley and Vanilla leaves compared to the monolayer control. n=3, $p<0.05$, One-way ANOVA followed by Dunnett's multiple comparisons test.

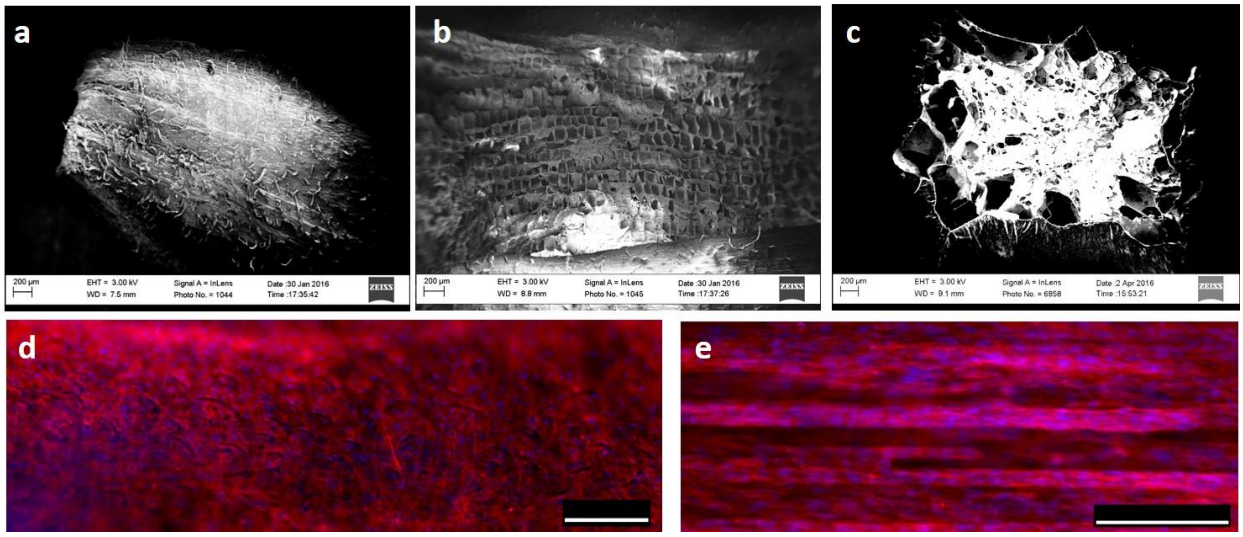

Figure S14: Cells behave differently in different regions of solenostemon stems: a-c, SEM micrographs of respectively the surface (a), a side-view (b) and a cross-section (c) of solenostemon stems. **d-e,** Rhodamine-phalloidine staining of actin filaments (red) and dapi staining of nuclei (blue) of hDF growing respectively on the surface (d) or within (e) solenostemon stems. Cells growing on the stem's surface appeared to have a random orientation (d) while cells growing within the stem (e) seemed to align to the stem's topography. Scalebars 250 µm.